

Are your MRI contrast agents cost-effective?

Learn more about generic Gadolinium-Based Contrast Agents.



**FRESENIUS
KABI**

caring for life

AJNR

Topographical Distribution of Pontocerebellar Microbleeds

Seung-Hoon Lee, Seon-Joo Kwon, Ki Soon Kim,
Byung-Woo Yoon and Jae-Kyu Roh

AJNR Am J Neuroradiol 2004, 25 (8) 1337-1341
<http://www.ajnr.org/content/25/8/1337>

This information is current as
of April 10, 2024.

Topographical Distribution of Pontocerebellar Microbleeds

Seung-Hoon Lee, Seon-Joo Kwon, Ki Soon Kim, Byung-Woo Yoon, and Jae-Kyu Roh

BACKGROUND AND PURPOSE: Microbleeds (MBs) visualized by use of T2*-weighted gradient-echo MR imaging are pathologic blood-breakdown products after tiny cerebral hemorrhages. The topographic distribution of the lesions has not been compared with that of symptomatic intracerebral hemorrhage (ICH). The purpose of this study was to evaluate the distribution of MBs in the pontocerebellar region and to compare it with the distribution of ICHs reported in the literature.

METHODS: We examined 164 consecutive hypertensive patients with ischemic infarction or spontaneous ICH over a 1-year period. Two experienced neuroradiologists assessed cerebral localization of MBs without prior knowledge of the clinical information and in consensus. After obtaining 16 standard axial brain images, we analyzed the anatomic locations and the vascular territories of the MBs in the pontocerebellar area.

RESULTS: We detected 374 pontocerebellar MBs in 40 patients (8.1 ± 12.7). Pontine MBs showed a significant predilection for the central portion (middle part along the axial plane, 3.4 ± 4.9 [$P < .01$]; medial part along the coronal plane, 3.4 ± 4.1 [$P < .01$]) and mostly belonged to the territory of the anteromedial group arising from the basilar artery. Cerebellar MBs had a frequent distribution around the dentate nucleus, occurring significantly more in the lower half, in the medial part (3.4 ± 4.6 ; $P < .01$), and in the middle part along the axial plane (4.8 ± 7.0 ; $P < .01$).

CONCLUSION: These findings were similar to the topography of ICH described in the literature. Our results suggest that MBs may be a lesional marker for ICH.

T2*-weighted gradient-echo (GE) MR imaging is a sensitive method for detecting small hemorrhage or calcification by their magnetic susceptibility effects (1). Microbleeds (MBs) visualized on GE images are usually caused by chronic hypertension (2–4) or cerebral amyloid angiopathy (5–7), and they are closely associated with old age (2); a low concentration of total cholesterol (4); and asymptomatic cerebral lesions, such as lacunae or leukoaraiosis (2, 8–11). Recently, MBs were pathologically demonstrated as a past extravasation of blood (3, 12), and a close relationship with intracerebral hemorrhage (ICH) has been reported (10). Therefore, some have suggested that MBs may precede or be a risk factor for ICH

(13–16). However, to be a lesional marker of ICH, the specific locations of MBs should be topographically similar to those of ICHs.

The aim of this study was to analyze the topography of MBs on the basis of the anatomic classification of the regions and the arterial territories and to compare the resulting topography with the locations of ICHs reported in the literature. We did not analyze the association in the supratentorial region, wherein ICHs have heterogeneous etiologies. Instead, we confined the MBs to the pontocerebellar region, for which hypertension is the most important risk factor.

Methods

Patients

We examined 164 consecutive hypertensive patients with ischemic infarction or spontaneous ICH between March 2000 and February 2001. All patients had acute stroke, which was identified by the clinical history and with the use of diffusion-weighted imaging or CT. The initial study population consisted of patients who underwent brain MR imaging including gradient echo (GE) sequences. Patients were ineligible if they had small hemorrhagic lesions of known or presumed pathogenesis (eg, lesions due to head trauma or surgery, current anticoagulant therapy, systemic neoplasm or brain tumor, arteriovenous

Received October 13, 2003; accepted after revision January 13, 2004.

From the Department of Neurology, Seoul National University and Neuroscience Research Institute, SNUMRC and Clinical Research Institute, Seoul National University Hospital (S.-H.L., S.-J.K., B.-W.Y., J.-K.R.), and the Department of Preventive Medicine, Chosun University College of Medicine, Gwangju (K.S.K.), Korea.

Correspondence to: Jae-Kyu Roh, Department of Neurology, Seoul National University Hospital, 28 Yongon-dong, Jongno-gu, Seoul, 110–744, Korea.

malformation, cavernous angioma, chronic liver disease, or other systemic coagulation dysfunction).

Major vascular risk factors were identified on the basis of medical history and laboratory findings. Leukoaraiosis was evaluated by means of T2-weighted spin-echo MR imaging and classified into four grades (17): 1) absent, no abnormality, or minimal periventricular hyperintensities in the form of caps confined exclusively to the anterior horns or rims lining the ventricles; 2) punctate hyperintensities in both the anterior and posterior horns of the lateral ventricles or periventricular unifocal patches; 3) early, multiple, confluent, hyperintense, periventricular punctate lesions, and their early confluence; and 4) multiple, confluent areas of high signal intensity reaching confluence in the periventricular region. Intracranial large-artery diseases were determined by means of MR angiography and defined as being present if >50% luminal narrowing was found in the intracranial internal carotid, anterior cerebral, middle cerebral, posterior cerebral, basilar, or intracranial vertebral arteries.

MR Imaging

MR images were obtained with a 1.5-T superconducting magnet (Signa, GE Medical Systems, Milwaukee, WI), and consisted of axial GE and T2-weighted spin-echo imaging and MR angiography. For the analysis of the GE MR images, the brain was imaged with a section thickness of 6 mm and a 2-mm intersection gap, producing 16 standard axial images. GE MR images were obtained in the axial plane parallel to the anterior commissure–posterior commissure line, with a TR/TE/NEX of 500/15/2–4, a flip angle of 20°, and a matrix of 256 × 192. Axial T2-weighted spin-echo sequences (TR/TE, 5000/110; section thickness, 6 mm; gap width, 2 mm) were used to grade leukoaraiosis. MR angiography (3D time-of-flight sequence; 30/6.9/32; flip angle, 20°; field of view, 220 × 170 mm; matrix size, 256 × 160; section thickness, 1.4 mm; no gap) was performed to analyze intracranial large-artery diseases.

Localization of MBs

MBs were observed as homogeneous, round lesions with loss of signal intensity and a diameter of up to 5 mm on the GE images. Hypointense lesions in the subarachnoid space were considered likely to represent adjacent pial blood vessels and therefore were not included.

Two experienced neurologists (S.-H.L., S.-J.K.) assessed the parenchymal localization of MBs by consensus, without prior knowledge of the clinical information. Pontocerebellar location was subdivided according to the anatomic locations or vascular territories. We compared the total number of MBs in each area. Localization of MBs was based on the templates that Tatu et al proposed (18). Of the 16 standard sections obtained in this study, five sections (the first to the fifth) were used in the analysis of the cerebellum, and three sections (the second to the fourth) were used in the analysis of the pons. The midbrain and medulla were excluded from this analysis on account of the extremely low incidence of MBs in these areas. The anatomic location in the pontocerebellar area was classified into anterior, middle, and posterior thirds along the sagittal plane and divided into lateral, middle, and medial thirds along the coronal plane. The arterial territories of the pons were grouped into those supplied by the anteromedial group arising from the basilar artery, those supplied by the anterolateral group arising from the basilar artery, those supplied by the lateral group arising from the basilar artery and from the anterior inferior cerebellar artery, and those supplied by the posterior group arising from the superior cerebellar artery. The cerebellar territories consisted of those supplied by the medial branches of the posterior inferior cerebellar artery, those supplied by the lateral branches of the posterior inferior cerebellar artery, those supplied by the anterior inferior cerebellar artery, those supplied by the lateral branches of the superior cerebellar

artery, and those supplied by the medial branches of the superior cerebellar artery.

Statistical Analysis

Unpaired *t* tests and Pearson χ^2 tests were used to compare the incidence of the demographic, clinical, and morphologic variables. The frequency of MBs in the various groups was compared by using the Pearson χ^2 tests. To compare the mean number of MBs in the different regions, the Mann-Whitney *U* test was used, because the numbers of MBs were not distributed normally (Kolmogorov-Smirnov test; $P < .001$). $P < .05$ was considered to indicate a statistically significant difference. Statistical analysis was performed with SPSS software version 10.0 (SPSS, Chicago, IL).

Results

Baseline Data

A total of 164 hypertensive patients with an ischemic infarct or spontaneous ICH were examined by using GE sequences. Their ages ranged from 33 to 92 years (mean, 64.6 ± 9.2 years), and they included 68 women and 96 men. Among the patients, 113 (68.9%) had an ischemic stroke, and 51 (31.1%) had a hemorrhagic stroke. Pontocerebellar MBs were detected in 46 (28.0%). The total number of pontocerebellar MBs evaluated in this study was 374 (8.1 ± 12.7 per patient). Table 1 provides a comparison of demographic variables and vascular risk factors between patients with MBs and those without MBs. Patients with MBs in the whole brain area had a lower prevalence of heart disease and large-artery disease; this finding was not observed in the comparison between patients with pontocerebellar MBs and those without these MBs. Leukoaraiosis and ICH were more common in patients with MBs than in the others.

Pons

We identified 40 patients (24.4%) with MBs in the pons, and 197 MB lesions were found in this region (4.9 ± 6.4). By visual estimation, the lesions seemed to be mainly distributed in the central portion of the pons (Figs 1 and 2). Anatomic analysis revealed a regional difference in the sagittal, axial, and coronal planes in the incidence of the MBs. Significant differences in the mean number of MBs were also observed along the axial and coronal planes but not along the sagittal plane (Table 2). Significantly higher numbers of MBs were observed in the middle part along the axial plane (3.4 ± 4.9 ; anterior part, 1.3 ± 2.2 ; posterior part, 0.3 ± 0.7) and in the medial part along the coronal plane (3.4 ± 4.1 ; median part, 1.2 ± 2.3 ; lateral part, 0.3 ± 0.9). Analysis based on the arterial territories showed a regional difference (Table 3), with 139 lesions (70.6%) in the territory of the anteromedial group arising from the basilar artery, 42 lesions (21.3%) in the anterolateral group territory, 16 lesions (8.1%) in the lateral group territory, and no lesions in the posterior group territory. The mean number was higher in the anteromedial group territory than in the other territories (3.4 ± 4.1 ; antero-

TABLE 1: Demographic data, vascular risk factors, and MR imaging findings in patients with and those without microbleeds

Data	Whole-Brain MB		P Value	Pontocerebellar MB		P Value
	Present (n = 98)	Absent (n = 66)		Present (n = 46)	Absent (n = 118)	
Demographic data						
Age	64.9 ± 9.3	64.2 ± 9.1	.62*	65.5 ± 10.3	64.2 ± 8.8	.43*
Male/Female (%)	60.2/39.8	56.1/43.9	.71†	67.4/32.6	55.1/44.9	.21†
Risk factors						
Diabetes (%)	25.5	24.2	>.99†	23.9	25.4	>.99†
Smoking (%)	30.6	31.8	>.99†	37.0	28.8	.41†
Cardiac disease (%)	7.1	25.8	<.01†	6.5	17.8	.09†
Cholesterol level (mg/dL)	185.2 ± 36.0	188.0 ± 48.2	.67*	187.7 ± 40.0	185.7 ± 41.8	.78*
Previous stroke (%)	33.7	21.2	.12†	34.8	26.3	.37†
Imaging findings						
Large-artery disease (%)	24.5	48.5	<.01†	23.9	38.1	.12†
Leukoaraiosis (%)‡	50.0	9.1	<.01†	63.0	22.0	<.01†
ICH (%)	37.8	21.2	.04†	47.8	24.6	<.01†

Note.—The mean ± SD was used to compare the non-MB and MB groups.

* Student *t* test.

† Pearson χ^2 test.

‡ Leukoaraiosis includes only early confluent or confluent abnormalities.

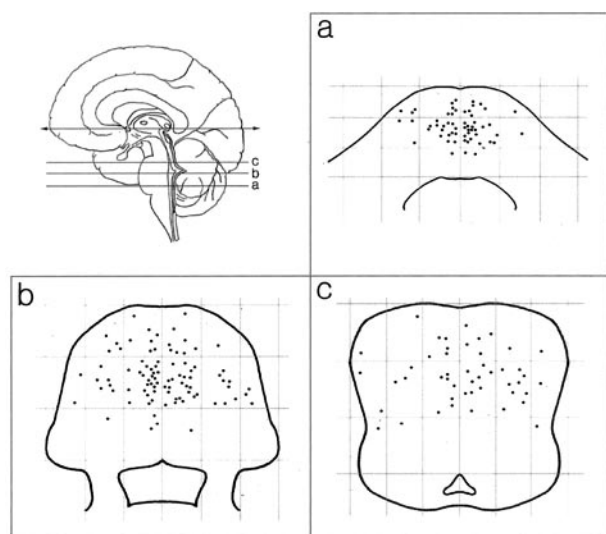


FIG 1. Topography of MBs in the pons. MBs were most commonly observed in the central portion of the midpons level.

lateral group territory, 1.1 ± 1.9 ; lateral group territory, 0.4 ± 1.1).

Cerebellum

Twenty-nine patients (17.7%) had a total of 177 MB lesions in the cerebellum (6.1 ± 9.1 ; maximum, 39). We noted a frequent distribution around the dentate nucleus. The anatomic distribution of the MBs in the cerebellum varied significantly between the sagittal, axial, and coronal planes. The lesions occurred significantly more often in the middle-inferior part along the sagittal plane (middle part, 2.2 ± 3.9 ; inferior part, 3.4 ± 5.0 ; superior part, 0.5 ± 1.2), in the middle part along the axial plane (4.8 ± 7.0 ; anterior part, 1.0 ± 2.2 ; posterior part, 0.4 ± 0.7), and in the medial part along the coronal plane (3.4 ± 4.6 ; median part, 2.4 ± 4.8 ; lateral part, 0.3 ± 0.7) than in

other parts. In the analysis based on the arterial territories, there were 20 lesions (11.3%) in the territory of the medial branches of superior cerebellar artery, 55 (31.0%) in the territory of the lateral branches, 18 (10.2%) in the territory of the anterior inferior cerebellar artery, 47 (26.6%) in the territory of the medial branches of posterior inferior cerebellar artery, and 37 (20.9%) in the territory of the lateral branches. The mean number of lesions was not significantly different (territory of the medial branches of superior cerebellar artery, 0.7 ± 1.3 ; territory of the lateral branches of superior cerebellar artery, 1.9 ± 3.7 ; territory of the anterior inferior cerebellar artery, 0.6 ± 1.8 ; territory of the medial branches of posterior inferior cerebellar artery, 1.6 ± 2.4 ; territory of the lateral branches of posterior inferior cerebellar artery, 1.3 ± 2.0).

Discussion

MBs are usually identified with the use of GE sequences that depict the paramagnetic signal intensity of hemosiderin deposits produced by the T2* effect (1). Pathologically, these lesions are previous microhemorrhages resulting from advanced fibrohyalinized arterioles (3, 12), and they therefore signify the presence of bleeding-prone microangiopathy in hypertensive patients. Because the vascular risk factors and pathologic findings are similar in MBs and ICH, some have proposed that MBs might be a causal factor for ICH in hypertensive patients. ICH generally results from the expansion of a hemorrhage after arteriolar rupture, and so it is somewhat difficult to locate the vessel that ruptured first. On the other hand, MBs are small lesions that are hardly detectable with conventional CT scanning and MR imaging. They can provide a means of analyzing the location of the rupture site through the use of the GE sequences. In this study, we examined 374 MB lesions in 164 consecutive patients with acute stroke. The present

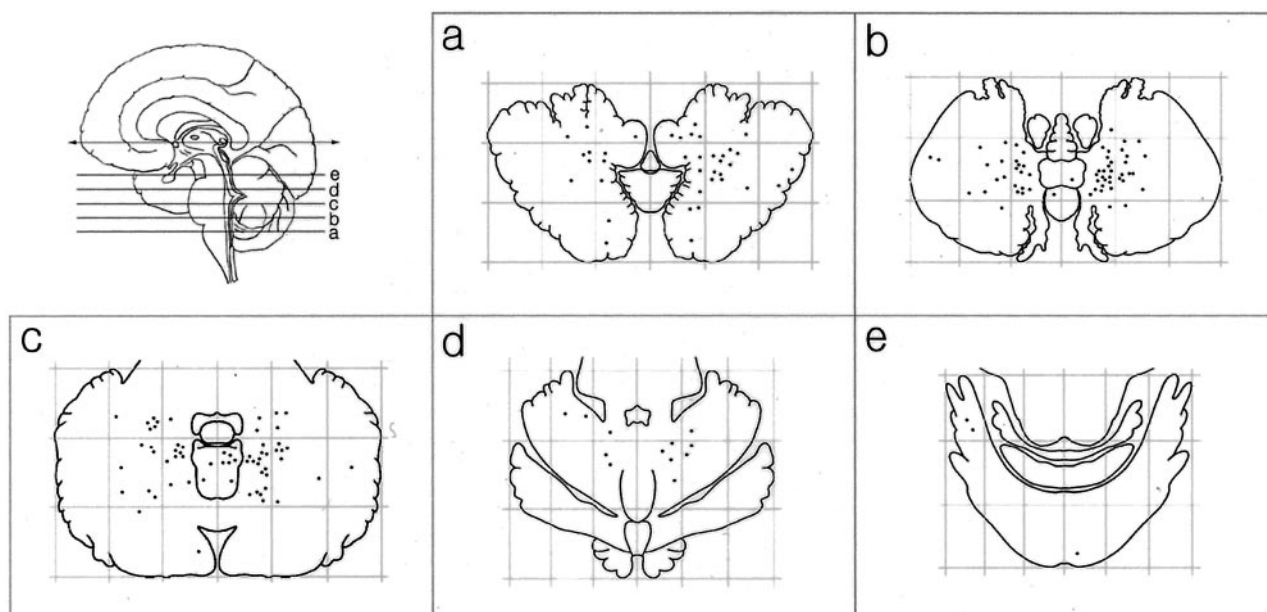


FIG 2. Topography of MBs in the cerebellum. Cerebellar MBs were crowded around the dentate nucleus in the lower half of the cerebellum.

TABLE 2: Analysis of MB location in the infratentorial area according to anatomic division

Direction and Comparison	P Value*	
	Pons	Cerebellum
Rostrocaudal		
Superior vs mid	.07	.02
Superior vs inferior	.28	<.01
Mid vs inferior	.46	.08
Anteroposterior		
Anterior vs mid	<.01	<.01
Anterior vs posterior	<.01	.56
Mid vs posterior	<.01	<.01
Mediolateral		
Medial vs median	<.01	.03
Medial vs lateral	<.01	<.01
Median vs lateral	.02	<.01

* The Mann-Whitney *U* test was used for the comparisons.

findings can be summarized as follows. First, the central part corresponding to the territory of the antero-medial group in the arterial classification was the most common location for the 197 pontine lesions. Second, cerebellar MBs ($n = 177$) were seen mostly around the dentate nucleus in the lower half of the cerebellum.

In general, pontine hematoma occurs in the form of a massive hemorrhage, usually in the midpons at the junction of the basis pontis and the tegmentum, which frequently spreads rostrally into the midbrain (19, 20). Our study showed that the MBs were distributed in the central portion of the pons. Regarding the vascular supply to the pons, the largest penetrating arteries enter medially, arise perpendicular to the basilar artery, and then follow a course from the base to the tegmentum. Other small, penetrating arteries originate from the short and long circumferential

TABLE 3: Analysis of MB location in the infratentorial area according to vascular territory

Location and Comparison	P Value*
Pons	
AMB vs ALB	<.01
AMB vs LB	<.01
ALB vs LB	.03
Cerebellum	
MSCA vs LSCA	.048
MSCA vs AICA	.39
MSCA vs MPICA	.052
MSCA vs LPICA	.08
LSCA vs AICA	<.01
LSCA vs MPICA	.90
LSCA vs LPICA	.84
AICA vs MPICA	<.01
AICA vs LPICA	<.01
MPICA vs LPICA	.69

Note.—AICA indicates anterior inferior cerebellar artery; ALB, anterolateral group from the basilar artery; AMB, anteromedial group from the basilar artery; LB, lateral group from the basilar artery and anterior inferior cerebellar artery; MSCA, medial branches of the superior cerebellar artery; LPICA, lateral branches of the posterior inferior cerebellar artery; LSCA, lateral branches of the superior cerebellar artery; and MPICA, medial branches of the posterior inferior cerebellar artery.

* The Mann-Whitney *U* test was used for the comparisons.

vessels and enter more laterally; they also follow a course from the base to the tegmentum. We found that the number of MBs was markedly higher in the territory of the anteromedial group; this result is consistent with the prior report by Silverstein (19), who analyzed 50 cases of pontine hemorrhage, 28 of which were massive central hemorrhages presumably arising from large paramedian penetrators.

Cerebellar hematoma appears with a frequency variously reported between 5–15% (21, 22). In this

case, the hematoma collects around the dentate and spreads into the hemispheric white matter, often extending into the cavity of the fourth ventricle as well. In this study, the prevalence of cerebellar MBs was 8.1% ($n = 177$). The lesions were intensively located around the dentate nucleus in the lower half of the cerebellum; this finding is closely correlated with the results of previous studies (22–24). It has long been understood that this area is particularly fragile, because the long, penetrating branches of the SCA are found around the dentate nucleus; these are anastomosed with cerebellar cortical arteries that supply the subcortical area after penetrating the cortex perpendicularly. In terms of the vascular territories, our study did not reveal the most common location of MBs; this difficulty might be associated with the complexity of the vascular supply around the dentate nucleus.

Conclusion

Our results confirmed that the topography of pontocerebellar MBs is strikingly similar to the topography of ICH described in the literature. These findings may provide evidence to support the hypothesis that asymptomatic MBs constitute a warning marker for future incidences of ICH. Our data on the locations of MBs should be helpful if and when a prospective study on the relationship between MBs and ICH is performed in the future.

References

1. Roob G, Fazekas F. **Magnetic resonance imaging of cerebral microbleeds.** *Curr Opin Neurol* 2000;13:69–73
2. Roob G, Schmidt R, Kapeller P, Lechner A, Hartung HP, Fazekas F. **MRI evidence of past cerebral microbleeds in a healthy elderly population.** *Neurology* 1999;52:991–994
3. Tanaka A, Ueno Y, Nakayama Y, Takano K, Takebayashi S. **Small chronic hemorrhages and ischemic lesions in association with spontaneous intracerebral hematomas.** *Stroke* 1999;30:1637–1642
4. Lee SH, Bae HJ, Yoon BW, Kim H, Kim DE, Roh JK. **Low concentration of serum total cholesterol is associated with multifocal signal loss lesions on gradient-echo magnetic resonance imaging: analysis of risk factors for multifocal signal loss lesions.** *Stroke* 2002;33:2845–2849
5. Greenberg SM. **Cerebral amyloid angiopathy: prospects for clinical diagnosis and treatment.** *Neurology* 1998;51:690–694
6. Greenberg SM, O'Donnell HC, Schafer PW, Kraft E. **MRI detection of new hemorrhages: potential marker of progression in cerebral amyloid angiopathy.** *Neurology* 1999;53:1135–1138
7. Greenberg SM, Rosand J. **Outcome markers for clinical trials in cerebral amyloid angiopathy [Suppl 1].** *Amyloid* 2001;8:56–60
8. Lee SH, Bae HJ, Ko SB, Kim H, Yoon BW, Roh JK. **A Comparative Analysis of the Spatial Distribution and Severity of Cerebral Microbleeds and Old Lacunes.** *J Neurol Neurosurg Psychiatry*. 2004; 75:423–427
9. Kwa VI, Franke CL, Verbeeten B Jr, Stam J. **Silent intracerebral microhemorrhages in patients with ischemic stroke: Amsterdam Vascular Medicine Group.** *Ann Neurol* 1998;44:372–377
10. Roob G, Lechner A, Schmidt R, Flooh E, Hartung HP, Fazekas F. **Frequency and location of microbleeds in patients with primary intracerebral hemorrhage.** *Stroke* 2000;31:2665–2669
11. Kato H, Izumiyama M, Izumiyama K, Takahashi A, Itoyama Y. **Silent cerebral microbleeds on T2*-weighted MRI: correlation with stroke subtype, stroke recurrence, and leukoaraiosis.** *Stroke* 2002;33:1536–1540
12. Fazekas F, Kleinert R, Roob G, et al. **Histopathologic analysis of foci of signal loss on gradient-echo T2*-weighted MR images in patients with spontaneous intracerebral hemorrhage: evidence of microangiopathy-related microbleeds.** *AINR Am J Neuroradiol* 1999;20:637–642
13. Lee SH, Bae HJ, Kwon SJ, et al. **Cerebral microbleeds are regionally associated with intracerebral hemorrhage.** *Neurology*. 2004;62: 72–76
14. Kidwell CS, Saver JL, Carneado J, et al. **Predictors of hemorrhagic transformation in patients receiving intra-arterial thrombolysis.** *Stroke* 2002;33:717–724
15. Nighoghossian N, Hermier M, Adeleine P, et al. **Old microbleeds are a potential risk factor for cerebral bleeding after ischemic stroke: a gradient-echo T2*-weighted brain MRI study.** *Stroke* 2002;33:735–742
16. Fan YH, Zhang L, Lam WW, Mok VC, Wong KS. **Cerebral microbleeds as a risk factor for subsequent intracerebral hemorrhages among patients with acute ischemic stroke.** *Stroke* 2003;34:2459–2462
17. Fazekas F, Chawluk JB, Alavi A, Hurtig HI, Zimmerman RA. **MR signal abnormalities at 1.5 T in Alzheimer's dementia and normal aging.** *AJR Am J Roentgenol* 1987;149:351–356
18. Tatu L, Moulin T, Bogousslavsky J, Duvernoy H. **Arterial territories of human brain: brainstem and cerebellum.** *Neurology* 1996;47:1125–1135
19. Silverstein A. **Primary pontile hemorrhage: a review of 50 cases.** *Confin Neurol* 1967;29:33–46
20. Nakajima K. **Clinicopathological study of pontine hemorrhage.** *Stroke* 1983;14:485–493
21. Freeman RE, Onofrio BM, Okazaki H, Dinapoli RP. **Spontaneous intracerebellar hemorrhage. Diagnosis and surgical treatment.** *Neurology* 1973;23:84–90
22. Heros RC. **Cerebellar hemorrhage and infarction.** *Stroke* 1982;13:106–109
23. Norris JW, Eisen AA, Branch CL. **Problems in cerebellar hemorrhage and infarction.** *Neurology* 1969;19:1043–1050
24. Ott KH, Kase CS, Ojemann RG, Mohr JP. **Cerebellar hemorrhage: diagnosis and treatment: a review of 56 cases.** *Arch Neurol* 1974; 31:160–167